Applied Physics Letters ARTICLE pubs.aip.org/aip/apl

Anisotropic creep velocity of Dzyaloshinskii domain walls

Cite as: Appl. Phys. Lett. **124**, 092403 (2024); doi: 10.1063/5.0191540
Submitted: 14 December 2023 · Accepted: 2 February 2024 ·
Published Online: 26 February 2024

Tchilabalo Pakam,[1,a)] Assiongbon Adanlété Adjanoh,[1] Serge Dzo Mawuefa Afenyiveh,[1] Jan Vogel,[2] Stefania Pizzini,[2,a)] and Laurent Ranno[2]

AFFILIATIONS

[1]Laboratoire Matériaux, Energies Renouvelables et Environnement, Département de Physique, Faculté des Sciences et Techniques, Université de Kara, 404 Kara, Togo
[2]Institut Néel, University Grenoble Alpes, CNRS, 38042 Grenoble, France

[a)]**Authors to whom correspondence should be addressed:** pakamtchilaba@gmail.com and stefania.pizzini@neel.cnrs.fr

ABSTRACT

We have measured the field-driven velocity of chiral Néel domain walls (DWs) stabilized by the Dzyaloshinskii–Moriya interaction (DMI) in a Pt/Co/Ta/Pt film with perpendicular magnetic anisotropy. A simple model based on the universal creep theory allows us to describe the anisotropic propagation of a DW along the contour of a bubble domain, driven by an out-of-plane field in the presence of a static in-plane field. This model is used to obtain the DMI constant from the measurement of the DW propagation with only one value of the in-plane field, simplifying the existing method relying on several measurements. The DMI constant extracted from the model is in good agreement with independent measurements.

The manipulation of spin textures, such as domain walls (DWs), does not only rely on the application of a magnetic field. Spin polarized electric currents[1] or more recently pure spin currents[2–4] have been shown to efficiently drive DWs. At the same time, beyond the well-known interface magnetic anisotropy generated in ultra-thin films, an interface-induced non collinear exchange, the Dzyaloshinskii–Moriya interaction (DMI) that stabilizes homochiral domain walls, can sometimes be evidenced when the magnetic system lacks inversion symmetry.[5,6] Brillouin light Scattering is one of the few direct methods to obtain the DMI amplitude D_i.[7,8] More often the DMI is estimated from evaluating the effective DMI field it generates, through the measurement of the anisotropic propagation of DWs.[9]

In this work, we provide a description of the DW velocity of a circular magnetic domain driven by an out-of-plane magnetic field H_z in the presence of an in-plane magnetic field H_x. The determination of D_i is based on the classical model proposed by Je *et al.*,[9] who showed that the presence of H_x modifies the DW energy and therefore the DW velocity in the creep regime. An H_x field with a component parallel/antiparallel to the DW magnetization direction will decrease/increase the DW energy and increase/decrease the DW velocity. In the presence of Néel walls stabilized by DMI, an anisotropic DW propagation is, therefore, expected. The DW velocity is shown to reach a minimum when $H_x = -H_{DMI}$, where $\mu_0 H_{DMI} = \frac{D_i}{M_s \Delta}$ is the effective field that stabilizes Néel walls. Δ is the domain wall parameter and M_s the spontaneous magnetization. Experimentally, this method involves measuring DW velocities along the H_x direction for a range of H_x field values, up to fields evidencing a velocity minimum. More recently, Hartmann *et al.*[10] developed a more complex model for measuring H_{DMI}. This requires a detailed domain wall energy calculation and does not predict the minimum velocity for $H = -H_{DMI}$.

We propose a simple analytic model that describes the velocity profiles of the DWs as a function of their polar orientation θ in the plane. We then use this model to extract the DMI amplitude from the domain expansion with a single value of the applied field H_x.

Domain wall dynamics is well described using the Landau–Lifschitz–Gilbert (LLG) equation. This equation is implemented in micromagnetic models using a finite element description of the domains and domain walls. A more compact and analytical model is the $q - \phi$ model, which describes the domain wall as a rigid spin texture, where only the position q and the magnetization orientation ϕ in the DW center are time-dependent parameters. This model has been applied to describe the thermally activated creep regime as well as the flow and precessional regimes at larger fields.[11] The $q - \phi$ model can be extended to include the DMI contribution.

In the presence of defects, in the creep regime and in 2D geometry (thin films), the domain wall velocity follows a universal law, with

an exponential field dependence characterized by a critical exponent $\frac{1}{4}$ [Eq. (1)].[12–14] At constant temperature, the equation can be written in a more compact form introducing α and v_0,

$$v(H_z) = v_d e^{-\frac{kT_d}{kT}\left(\left(\frac{H_z}{H_d}\right)^{-1/4}-1\right)}, \qquad v(H_z) = v_0 e^{-\alpha H_z^{-1/4}}, \tag{1}$$

where T_d and H_d are the characteristic depinning temperature and field, respectively, and v_d is the DW velocity at the depinning field.

The presence of an in-plane field H_x can be included in Eq. (1), considering that the coefficient α depends on the H_x field only via the domain wall energy $\sigma(H_x)$,[9]

$$v(H_x, H_z) = v_0 e^{-\alpha\left(\frac{\sigma(H_x)}{\sigma(0)}\right)^{1/4} H_z^{-1/4}}. \tag{2}$$

For a circular domain, we define the angles θ and ϕ with respect to the in-plane field H_x: θ represents the domain wall propagation direction and ϕ the magnetization direction inside the DW (Fig. 1). $\Omega = \theta - \phi$ will give the Néel/Bloch character for the wall (Néel DW for $\Omega = 0, \pi$ and Bloch DW for $\Omega = \pm\pi/2$).

The domain wall energy $\sigma(H_x, \theta)$ can be obtained by minimizing the different terms that contribute to it: the Bloch term, the DMI term, and the Zeeman term associated with the H_x field and the demagnetizing term associated with the volume charges due to its Néel character,

$$\sigma(H_x, \theta, \phi) = 4\sqrt{AK_{eff}} - \pi|D_i|\cos(\Omega) - \pi\Delta M_s \mu_0 H_x \cos(\phi) + \frac{\ln(2)}{\pi} t\mu_0 M_s^2 \cos^2(\Omega), \tag{3}$$

where A is the exchange constant, K_{eff} is the effective anisotropy, D_i is the DMI constant, $\Delta = \sqrt{A/K_{eff}}$ is the domain wall parameter, t is the thickness of the magnetic layer, and M_s is its spontaneous magnetization.[15–17]

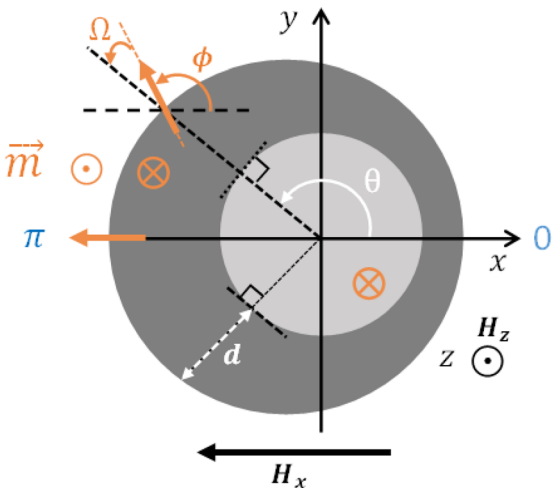

FIG. 1. Schematic representation of the expanding circular magnetic domain driven by an out-plane field (H_z) pulse in the presence of an in-plane field (H_x) and DMI. In light gray, the first circular domain nucleated with H_z (with $H_x = 0$) and in the dark gray the domain after propagation. The propagation direction of the DW is defined by θ, the angle between the DW normal of the first domain and the in-plane field direction. Magnetic moments $\vec{m}$ within the DW are represented as orange arrows. $\vec{m}$ is characterized by the angle ϕ with respect to the direction of H_x.

TABLE I. Sample quasi-static parameters. M_S is the spontaneous magnetization, K_{eff} the effective magnetic anisotropy constant, Δ is the DW parameter, and D_i the DMI strength.

M_S (MA/m)	A (pJ/m)	K_{eff} (kJ/m^3)	Δ (nm)	D_i (mJ/m^2)
1.2	16	339	4.4	-0.43 ± 0.05

For each θ and a given value of D_i, the minimization of $\sigma(H_x, \theta)$ gives the equilibrium value of ϕ. The DW velocity $v(H_x, H_z, \theta)$ can then be obtained using Eq. (2).

In the rest of our work, we will compare this model [Eq. (2)] with the experimental velocities and its correctness at determining the DMI amplitude. First, we will describe the experimental protocol used to generate the $v(H_x, \theta)$ data. Second, we will analyze the experimental velocities with the theoretical model.

The sample Pt(4 nm)/Co(0.8 nm)/Ta(0.32 nm)/Pt(2 nm) is deposited by DC magnetron sputtering on a Si/SiO_2 substrate with 3 nm of Ta buffer layer. The magnetic characterization is performed using polar Magneto-optical Kerr Effect Microscopy (PMOKE) and Superconducting Quantum Interference Device—Vibrating Sample Magnetometer (SQUID-VSM). The quasi-static parameters are collected in Table I. K_{eff} was obtained using $A = 16$ pJ/m, value used in the literature for Co layers with similar thicknesses.[18] The DW propagation regime is verified by measuring DW velocities v as a function of out-of-plane magnetic field (H_z). Figure 2 shows the velocity plot as a function of H_z. On the figure are plotted simultaneously v vs H_z and ln (v) vs $H_z^{-1/4}$. The linear dependence of ln(v) with $H_z^{-1/4}$ proves that DWs in this range of applied field propagate in the creep regime. The creep parameters v_0 and α are extracted from the fit to Eq. (1) and are $v_0 = (1 \pm 0.3)\ 10^{11}$ m/s and $\alpha = (12 \pm 1)\mathrm{T}^{1/4}$. The maximum amplitude of $\mu_0 H_z$ used for the measurement is 16.5 mT. This value leaves the DW propagation in the creep regime.

Domain imaging is performed using PMOKE microscopy. The protocol starts with the saturation of the magnetization in the

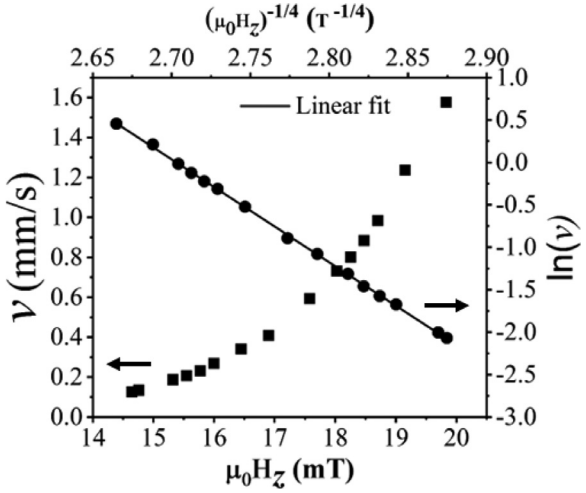

FIG. 2. Plot of the experimental domain wall velocity in the creep regime: v vs $\mu_0 H_z$ (black squares) and ln(v) vs $(\mu_0 H_z)^{-1/4}$ (black circles) together with the linear fit (black line) to Eq. (1).

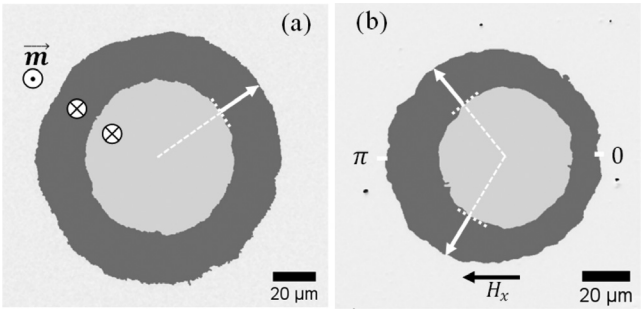

FIG. 3. Differential MOKE image representing the propagation of a DW driven by an out-of-plane magnetic field pulse $\mu_0 H_z = 16.5$ mT with $H_x = 0$ (a) and in the presence of an in-plane field $\mu_0 H_x = 43$ mT (b). In light gray is the first nucleated domain and in the dark gray the propagated domain.

out-of-plane direction by applying a H_z pulse larger than the saturation field. An opposite H_z field pulse is then applied to nucleate a circular magnetic domain. The corresponding image is recorded as image 1. The last step of the recording measurement consists in propagating the previously nucleated domain with a pulse of H_z in the presence or not of a constant and uniform in-plane field H_x. The image corresponding to this step is recorded as image 2. The images are then processed using the OpenCv(Cv2) Python library.[19] Image 2 is subtracted from image 1. Figure 3 shows the differential MOKE images measured without in-plane field (a) and with $\mu_0 H_x = 43$ mT (b). Next, the contours (representative of the DW positions) of the two domains are extracted using contour detection modules. The displacement of the DWs from the contour of the initial domain to the contour of the propagated domain is then used to determine the displacement $d(\theta)$. It should be noted that the first domain being circular, the normal to its surface is characterized by the angle θ. The DW velocity $v(H_x, \theta)$ is then extracted from the displacement $d(\theta)$ during the duration dt of the field pulse H_z, from the relation $d(\theta) = v(\theta)dt$.

When $H_x = 0$, the displacement should be isotropic. To confirm this, we measured the velocity along the entire contour of the magnetic domain. We have defined θ with respect to the positive x-direction passing through the center of the nucleated domain. On Fig. 4, $v(H_x = 0, \theta)$ evidences this isotropic velocity. The isotropic propagation also confirms that H_z is well aligned and has negligible IP component. This is useful in the analysis of DWs expansion in the presence of the IP field.

Applying an in-plane field leads to an anisotropic propagation of the DWs, highlighting the presence of DMI. The velocity in this case depends on the strength of H_x and the propagation angle, $v(H_x, \theta)$. Figure 4 represents the velocity profiles for different H_x values from 0 to 66 mT. For this study, we limited the maximum H_x value to 66 mT, for two reasons: first, for a higher field, the density of nucleated domains increases and an overlap between domains can appear; second, this prevents temperature rise due to electromagnets heating. In this limit, the precision of all the used H_x fields is estimated to be 3 mT.

Let us now check the agreement between the theoretical model and the experimental data. The theoretical model describes $v(H_x, \mu_0 H_z = 16.5\,\text{mT}, \theta)$. Using a guess value of D_i (in our case the one obtained in Ref. 18 for a sample with similar composition), the DW energy σ is minimized, numerically, resulting in an equilibrium

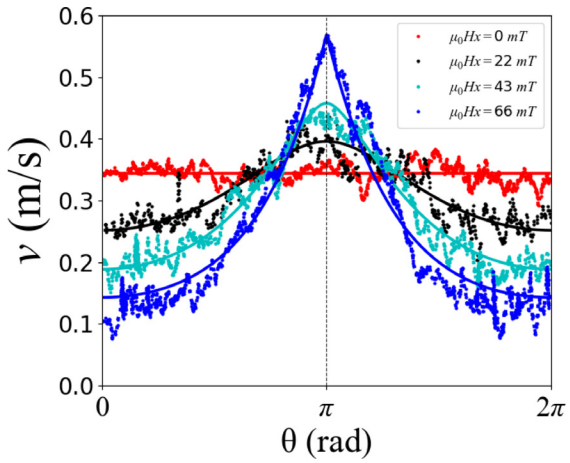

FIG. 4. Anisotropic DW velocity profiles measured for $\mu_0 H_z = 16.5$ mT with a range of in-plane field H_x (0, 22, 43, and 66 mT) and best fits obtained using the model $v(\theta, H_x, \mu_0 H_z = 16.5\,\text{mT})$.

value for ϕ for each angle θ. The resulting σ is then injected into Eq. (2) to obtain de DW velocity profile vs θ. v_0 and α are those deduced from the fit of the experimental velocities to the creep law [Eq. (1)]. Each $v(\theta, H_x)$ profile corresponding to a given H_x is then fitted by leaving both ϕ and D_i as free parameters. As can be seen in Fig. 4, the fits are all in good agreement with the data. The model describes correctly not only the minimum and maximum speeds but also the shape of the velocity curve as a function of the polar angle θ.

Fitting the full $v(\theta)$ curve reduces the fitting error compared to fitting only velocities in the $\theta = 0$ and π directions (along $\vec{H}_x$). The value of the DMI amplitude obtained from the fits of the experimental velocity curves depends very slightly on the H_x strength. The average value of D_i is -0.43 ± 0.05 mJ/m^2 giving an average H_{DMI} field of 83 ± 3 mT [Fig. 5(a)]. This DMI value is very close to that found in Ref. 18 for a very similar sample composition. On the other hand, since in our sample Ta is only a very thin dusting layer, D_i is smaller than the values found in the literature for Pt/Co/Ta trilayers with thicker Ta layers.[20]

The H_{DMI} value can be compared with that obtained with the classical method proposed by Je *et al.*[9] The DWs velocity at $\theta = 0$ measured as a function of the strength of H_x is shown in Fig. 5(b). From the fit of the curve using Eq. (3), the DMI field, corresponding to the H_x with the minimum speed, is determined to be $\mu_0 H_{DMI} = 84 \pm 5$ mT. This is in excellent agreement with the value obtained from the $v(\theta)$ fit.

In conclusion, we have proposed a method to extract the DMI value from the analysis of the anisotropic propagation of Néel domain walls as a function of their polar orientation. A simple analytic model based on the universal creep model allows describing the measured velocity profiles. The DMI amplitudes do not depend on the applied in-plane field and agree with the value extracted from the classical minimum velocity model. The advantage of this protocol is that it allows determining the DMI constant from the velocity measurement with a single H_x field. This method can be helpful in the case of large H_{DMI} fields difficult to reach experimentally, or in samples with small anisotropy where large in-plane fields give rise to a large density of nucleated domains.

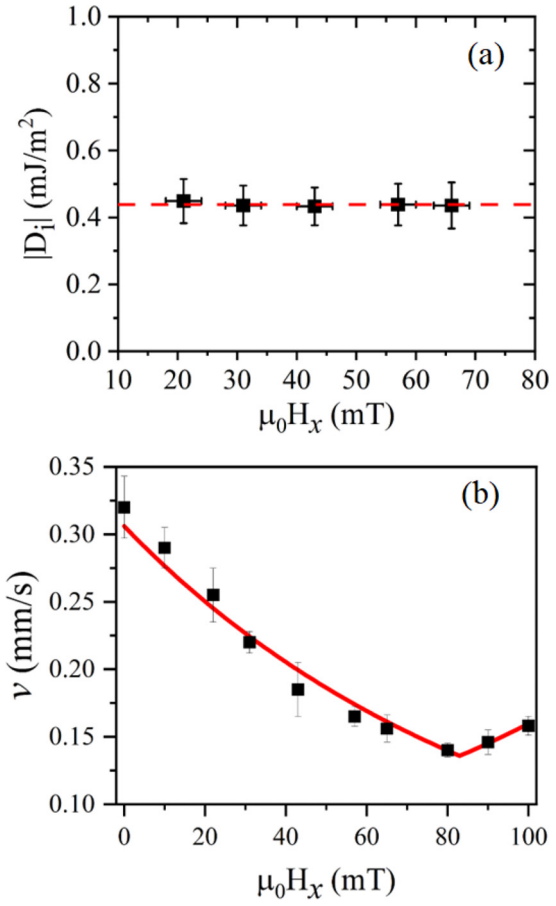

FIG. 5. (a) DMI constant D_i found from the fit of the experimental curves using Eq. (2), for different values of H_x (22, 32, 43, 56, and 66 mT). The red dash-line presents the average of D_i and (b) DW velocity measured as a function of H_x for $\theta = 0$ with $\mu_0 H_z = 16.5$ mT.

The authors acknowledge the financial support of Service de coopération et d'action culturelle-France au Togo (SCAC-Togo). We are also thankful to Eric Mossang for his assistance with XRD and XRR measurements and to Philippe David and David Barral for their assistance for sputtering deposition and fruitful discussions.

AUTHOR DECLARATIONS

Conflict of Interest

The authors have no conflicts to disclose.

Author Contributions

Tchilabalo Pakam: Conceptualization (equal); Data curation (equal); Formal analysis (equal); Investigation (equal); Methodology (equal); Project administration (equal); Resources (equal); Software (equal); Supervision (equal); Validation (equal); Visualization (equal); Writing – original draft (equal); Writing – review & editing (equal). **Assiongbon Adanlété Adjanoh:** Conceptualization (supporting); Formal analysis (equal); Investigation (equal); Methodology (equal); Resources (equal); Supervision (equal); Validation (supporting); Visualization (equal). **Serge Dzo Mawuefa Afenyiveh:** Formal analysis (equal); Investigation (equal); Methodology (equal); Validation (supporting); Visualization (equal). **Jan Vogel:** Conceptualization (equal); Data curation (equal); Formal analysis (equal); Investigation (equal); Methodology (equal); Project administration (equal); Resources (lead); Supervision (equal); Validation (equal); Visualization (equal). **Stefania Pizzini:** Data curation (equal); Formal analysis (equal); Investigation (equal); Methodology (equal); Project administration (equal); Resources (equal); Supervision (equal); Validation (equal); Visualization (equal); Writing – review & editing (equal). **Laurent Ranno:** Conceptualization (lead); Data curation (equal); Formal analysis (equal); Investigation (equal); Methodology (equal); Project administration (lead); Resources (equal); Software (equal); Supervision (equal); Validation (equal); Visualization (equal); Writing – original draft (supporting); Writing – review & editing (equal).

DATA AVAILABILITY

The data that support the findings of this study are available from the corresponding authors upon reasonable request.

REFERENCES

[1] L. Berger, "Exchange interaction between ferromagnetic domain wall and electric current in very thin metallic films," J. Appl. Phys. **55**, 1954 (1984).
[2] I. M. Miron, T. Moore, H. Szambolics, L. D. Buda-Prejbeanu, S. Auffret, B. Rodmacq, S. Pizzini, J. Vogel, M. Bonfim, A. Schuhl, and G. Gaudin, "Fast current-induced domain-wall motion controlled by the Rashba effect," Nat. Mater. **10**, 419 (2011).
[3] S. Emori, U. Bauer, S.-M. Ahn, E. Martinez, and G. S. D. Beach, "Current-driven dynamics of chiral ferromagnetic domain walls," Nat. Mater. **12**, 611 (2013).
[4] K.-S. Ryu, L. Thomas, S.-H. Yang, and S. Parkin, "Chiral spin torque at magnetic domain walls," Nat. Nanotechnol. **8**, 527 (2013).
[5] I. Dzialoshinskii, "Thermodynamic theory of weak ferromagnetism in antiferromagnetic substances," Sov. Phys. JETP **5**, 1259 (1957).
[6] T. Moriya, "Anisotropic superexchange interaction and weak ferromagnetism," Phys. Rev. **120**, 91 (1960).
[7] H. T. Nembach, J. M. Shaw, M. Weiler, E. Jué, and T. J. Silva, "Linear relation between Heisenberg exchange and interfacial Dzyaloshinskii–Moriya interaction in metal films," Nat. Phys. **11**, 825 (2015).
[8] K. Di, V. L. Zhang, H. S. Lim, S. C. Ng, M. H. Kuok, J. Yu, J. Yoon, X. Qiu, and H. Yang, "Direct observation of the Dzyaloshinskii-Moriya interaction in a Pt/Co/Ni film," Phys. Rev. Lett. **114**, 047201 (2015).
[9] S.-G. Je, D.-H. Kim, S.-C. Yoo, B.-C. Min, K.-J. Lee, and S.-B. Choe, "Asymmetric magnetic domain-wall motion by the Dzyaloshinskii-Moriya interaction," Phys. Rev. B **88**, 214401 (2013).
[10] D. M. F. Hartmann, R. A. Duine, M. J. Meijer, H. J. M. Swagten, and R. Lavrijsen, "Creep of chiral domain walls," Phys. Rev. B **100**, 094417 (2019).
[11] A. Thiaville and Y. Nakatani, "Domain-wall dynamics in nanowiresand nanostrips," in *Spin Dynamics in Confined Magnetic Structures III, Topics in Applied Physics*, edited by B. Hillebrands and A. Thiaville (Springer, Berlin, Heidelberg, 2006), pp. 161–205.
[12] S. Lemerle, J. Ferré, C. Chappert, V. Mathet, T. Giamarchi, and P. Le Doussal, "Domain wall creep in an Ising ultrathin magnetic film," Phys. Rev. Lett. **80**, 849 (1998).
[13] V. Jeudy, A. Mougin, S. Bustingorry, W. Savero Torres, J. Gorchon, A. B. Kolton, A. Lemaître, and J.-P. Jamet, "Universal pinning energy barrier for driven domain walls in thin ferromagnetic films," Phys. Rev. Lett. **117**, 057201 (2016).

[14]V. Jeudy, R. Díaz Pardo, W. Savero Torres, S. Bustingorry, and A. B. Kolton, "Pinning of domain walls in thin ferromagnetic films," Phys. Rev. B **98**, 054406 (2018).
[15]A. Thiaville, S. Rohart, É. Jué, V. Cros, and A. Fert, "Dynamics of Dzyaloshinskii domain walls in ultrathin magnetic films," Europhys. Lett. **100**, 57002 (2012).
[16]M. Heide, G. Bihlmayer, and S. Blügel, "Dzyaloshinskii-Moriya interaction accounting for the orientation of magnetic domains in ultrathin films: Fe/W (110)," Phys. Rev. B **78**, 140403 (2008).
[17]J. P. Pellegren, D. Lau, and V. Sokalski, "Dispersive stiffness of Dzyaloshinskii domain walls," Phys. Rev. Lett. **119**, 027203 (2017).
[18]J. P. Garcia, A. Fassatoui, M. Bonfim, J. Vogel, A. Thiaville, and S. Pizzini, "Magnetic domain wall dynamics in the precessional regime: Influence of the Dzyaloshinskii-Moriya interaction," Phys. Rev. B **104**, 014405 (2021).
[19]I. Culjak, D. Abram, T. Pribanic, H. Dzapo, and M. Cifrek, "A brief introduction to OpenCV," in *Proceedings of the 35th International Convention MIPRO* (IEEE, 2012), pp. 1725–1730.
[20]M. Kuepferling, A. Casiraghi, G. Soares, G. Durin, F. Garcia-Sanchez, L. Chen, C. H. Back, C. H. Marrows, S. Tacchi, and G. Carlotti, "Measuring interfacial Dzyaloshinskii-Moriya interaction in ultrathin magnetic films," Rev. Mod. Phys. **95**, 015003 (2023).